Turkish Computational and Theoretical Chemistry

Turkish Comp Theo Chem (TC&TC)

Volume(Issue): 7(1) – Year: 2022 – Pages: 1-13

e-ISSN: 2602-3237

https://doi.org/10.33435/tcandtc.1064768

Received: 29.01.2022 ***Accepted:*** 07.05.2022 *Research Article*

Theoretical study of the reaction mechanism between triphenylphosphine with dimethyl acetylenedicarboxylates in the presence of 2-mercapto thiazoline

Mohammad Zakarianezhad[a, 1] , Batoul Makiabadi[b], Seyede Samira Hosseini[a], Elham Zeydabadi[a]

[a]Department of Chemistry, Payam Noor University, Tehran, Iran
[b]Department of Chemical Engineering, Sirjan University of Technology, Sirjan, Iran

Abstract: In this research, the mechanism of the reaction between triphenylphosphine **R1** and dimethyl acetylenedicarboxylate **R2** was investigated in the presence of NH-acid, such as 2-mercapto thiazoline **R3** based on the quantum mechanical calculations. Theoretical studies performed for evaluation of the potential energy surfaces of all structures participated in the reaction mechanism. All structures were optimized at the B3LYP/6-311++g(d,p) levels. The first step of the reaction was recognized as a rate-determining step in the reaction mechanism. To check the effect of solvent on the potential energy surfaces, condensed phase calculations in acetone were carried out with the polarizable continuum model (CPCM). The natural bond orbital (NBO) method was applied for a better understanding of molecular interaction. Theoretical calculations were well able to explain the reason for the dominant of product **P(N)-*E*** over **P(N)-*Z***. The overall rate equation obtained shows the overall reaction rate constant depends on the concentration of **R1** and **R2** without dependence on the concentration of **R3**. The kinetic preference of path **I** over path **II**, the conversion of intermediates with a ***Z*-** to ***E*-** configuration along the kinetic path, and the high energy barrier of the **P(N)-*E*** to **P(N)-*Z*** conversion are the three main reasons for the preference of **P(N)-*E*** over **P(N)-*Z***, which is obtained using quantum calculation.

Keywords: *NH-acid, E- and Z-rotamers, Triphenylphosphine*

1. Introduction

Organophosphorus compounds have emerged as important reagents and intermediates in organic synthesis. these compounds are organic chemicals derived from phosphoric acids and their derivatives which have at least one carbon-phosphorus bond [1]. Thiols, amides or esters of phosphonic, phosphine, phosphoric or thiophosphoric acids with two additional organic side chains of the phenoxy, cyanide or thiocyanate group are organophosphorus compounds that have pesticidal properties [2]. Phosphorus ylids are an important group of these compounds that are used in the synthesis of products with biological and pharmaceutical activities [3-6]. Several methods have been developed for the preparation of phosphorus ylides. These ylides are usually prepared by treatment of a phosphonium salt with a base, with the salts usually prepared from the phosphine and an alkyl halide [7-11]. Michael addition of triphenylphosphine to acetylenic esters leads to reactive 1, 3-dipolar intermediate betaines. These unstable intermediates can be reacted by protic reagent such as NH-,CH, OH- or SH-acid to produce ylides [12-23]. Although some of these represent only one isomer, there are a significant number of phosphorus ions as a mixture of the two geometric isomers Z- and E-. These geometric isomers show the dynamic effect of 1H NMR, which provides good information about the interchangeable process of rotational isomers [24,25]. The 1H, 13C and 31P NMR analysis. Although useful information obtained through experimental methods, none of the spectrophotometric methods could provide useful information about the reason for the presence of rotational isomers and their conversion energy. The

[1] Corresponding Authors
e-mail: m.zakarianejad@yahoo.com & mzakarianejad@pnu.ac.ir

preference and frequency of each of these rotamers can be well determined by spectrophotometry. The thermodynamically stable product is thought to be the preferred product, but the quantum calculations performed in this project have shown well that the preference of a particular rotamer does not depend only on its thermodynamic stability, and kinetic stability can also play an important role in this regard. The isolated products from the reactions of triphenylphosphine R1, dimethyl acetylenedicarboxylate R2 and 2-mercapto thiazoline R3 phosphorus ylides which result from the initial addition of triphenylphosphine to the acetylenic ester and a concomitant protonation of the 1:1 adduct by 2-mercapto thiazoline. Then the positively charged ion is attacked by the 2-mercapto thiazolyl anion [26]. In the present work, the reaction between a kinetic study, including determining the preferred kinetic path, investigation of intermediate structures and transition states in the reaction path, determination of the kinetic and thermodynamic stability of products, recognition of rate-determining step, calculation of the reaction rate, and finally, identifying and confirming the reaction mechanism are the issues that have been first explored for the reaction in Fig. 1. A number of projects, including the theoretical and experimental study of chemical reaction kinetics, were completed [27-40].

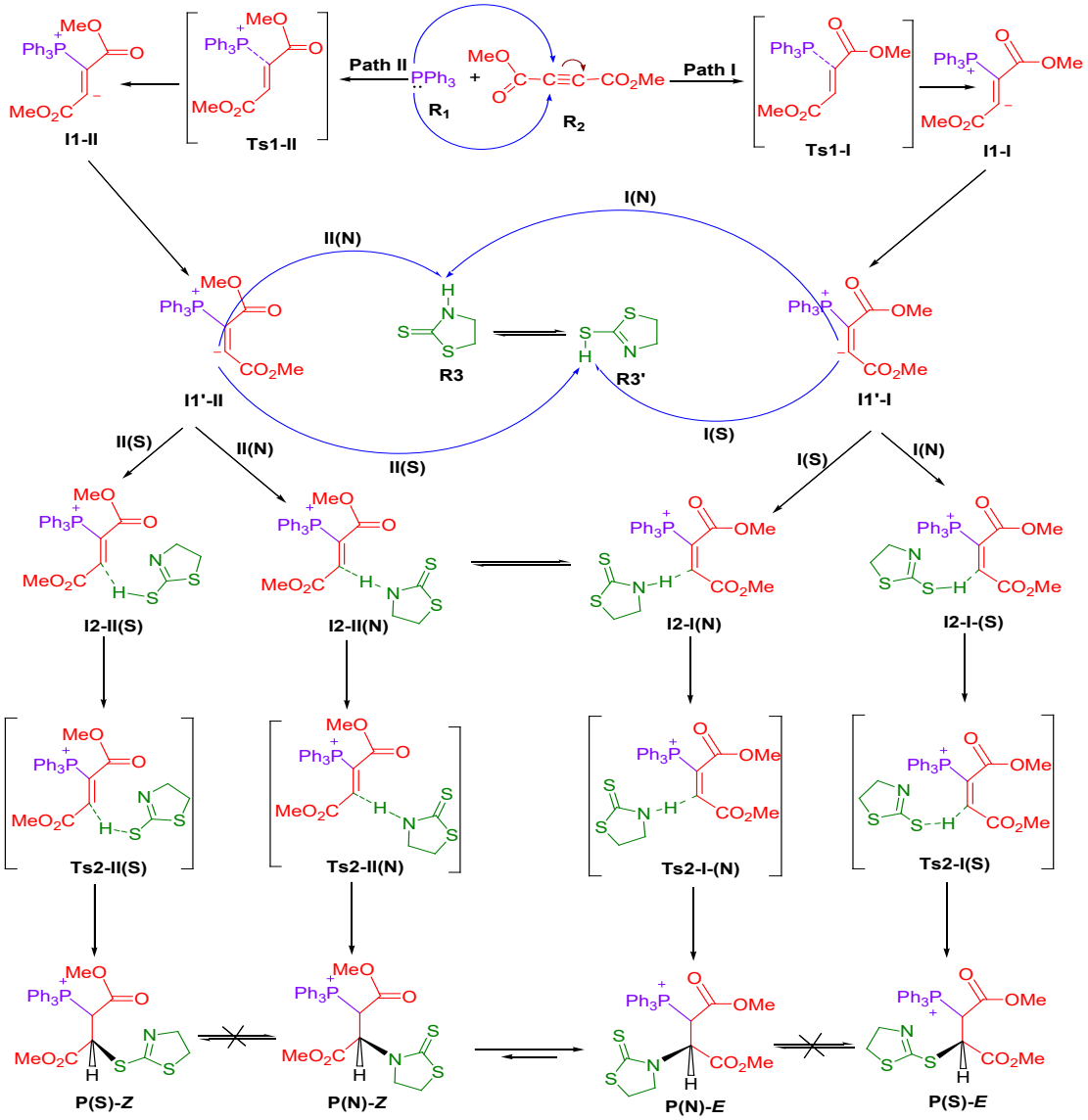

Figure 1. The reaction between triphenylphosphine R1, dimethyl acetylendicarboxylates R2, and 2-mercapto thiazoline R3 or R3' for the generation of stable phosphorus ylides P (P(N)-E and P(N)-Z)

2. Computational Method

All Geometrical structures were optimized at the B3LYP/6-311++G(d,p) level of theory using Gaussian 09 [41]. The corresponding frequencies of the structures were estimated at the same level of theory to check the stationary points without imaginary frequencies and the transition states with only one imaginary frequency. Also, the intrinsic reaction coordinate (IRC) approach [42,43] was performed to ensure that the given transition state connects with the corresponding reactants and products. Calculations have been carried out both in the gas phase and considering solvent effects (acetone) with the CPCM model [44-45]. Condensed phase calculations were carried out with the polarizable continuum model (PCM) [46]. Natural bond orbital (NBO) analysis was carried out at the B3LYP/6-311++G(d,p) level of theory using version 3.1 of the NBO package [47].

3. Results and discussion

3.1. The reaction kinetics in Path I

Nucleophilic proximity of atom P17 in triphenylphosphine **R1** to the atom C8 of dimethyl acetylenedicarboxylate **R2** in different directions leads to the formation of different kinetic pathways of **I** or **II** which respectively leads to the formation of products including two different isomers **P-*E*** and **P-*Z***. Optimized structures of all structures participant in the reaction mechanism in kinetic pathways **I** and **II** are shown in Figs. **2** and **3** and the energy diagram for the reaction is illustrated in Fig. **4**. This nucleophilic proximity on the pathway **I** cause the formation of intermediate **I1-I** through a transition state **Ts1-I**. This step of the reaction includes P17-C8 bond formation. A 180-degree rotation of the dihedral angle of C6-C8-C9-C10 in the conversion of **I1-I** to **I1'-I**, in addition to the stability of 9.59 (18.34) kJ/mol, will be accompanied by a suitable configuration for proximity to **R3** or **R3'**. The reactant **R3** (as NH-acid) can transform into its tautomeric form of **R3'** (as SH-acid) through an intermolecular proton transfer of H51 from N52 into S54, which is accompanied by a transition barrier of 157.34 (172.27) kJ/mol (Fig. **4**). This tautomerism will result in an instability of 41.42 (57.20) kJ/mol in structure **R3'** compared to **R3**. The interaction of **R3** or **R3′** with **I1′-I** is an important step that can pass two competitive kinetic paths of **I(N)** or **I(S)** and end up in stable products of **P(N)-*E*** or **P(S)-*E***. In the kinetic path **I(N)**, intermediate **I2-I(N)** is formed by hydrogen bond interactions of C9 in intermediate **I1'-I** and H51 atoms in the structure of **R3**. In the final step of this path, we witness the transfer of H51 to C9 in the structure of **Ts2-I(N)** and also the bond formation of N52-C9, which leads to the formation of the final product **P(N)-*E***. This step of the reaction is accompanied by a 27.20 (19.59) kJ/mol energy barrier and ends with a product with an energy of 13.97 (29.36) kJ/mol. In the competitive path of **I(S)**, intermediate **I2-I(S)** is formed by hydrogen bond interactions of C9 in intermediate **I1'-I** and H51 atoms in the structure of **R3'**. In the next step, we witness the transfer of H51 to C9 atom in the structure of **Ts2-I(S)** and the bond formation of S54-C9, which leads to the formation of product **P(S)-*E***. This step of the reaction is accompanied by a low energy barrier of 3.22 (1.81) kJ/mol and ends with a more stable product with an energy of -2.61 (0.10) kJ/mol. Examination of the energy levels in two competitive paths of **I(N)** and **I(S)** indicates that the kinetic path of **I(S)** with much less energy barrier than the path **I(N)** and ending up with a much more stable product of **P(S)-*E*** seems to be preferred kinetic path compared to the path **I(N)**, both kinetically and thermodynamically. Any conclusion in this regard depends on a more detailed study of tautomeric forms of **R3** and **R3'**. Examination of the energy levels of the thiolactam-thiolactone tautomerism in Fig. **5** shows a considerable stability of **R3** (as NH-acid) by -41.42 (-57.20) kJ/mol relative to **R3'**. This amount of stability indicates the predominant of **R3** over **R3'**. In addition, the high energy barrier of 157.34 (172.27) kJ/mol of the tautomerism indicates the impossibility of converting **R3** to **R3'** at ambient temperature. Considering that the reaction takes place at ambient temperature [26], it can be confirmed with great accuracy that the tautomeric form of **R3** is dominant at ambient temperature. With the results obtained, we must assume that the reaction proceeds through path **I(S)** as a more kinetically and thermodynamically preferred path and ends to the product **P(S)-*E***. The experimental results reported indicate that products **P(N)-*E*** and **P(N)-*Z*** are the only products of this reaction and products **P(S)-*E*** and **P(S)-*Z*** are not even reported

as minor products [26]. Starting the reaction in the competitive path **I(S)** requires an interaction of intermediate **I1'-I** with unstable reactant **R3'**, which for the above reasons is very unlikely to exist at ambient temperature. Therefore, the reaction prefers the 29.98(14.90) kJ/mol energy barrier in the intramolecular proton transfer in **Ts2-I(N)** over the 157.34 (172.27) kJ/mol energy barrier in the intramolecular proton transfer in **Ts(R3-R3')**. Therefore, the reaction ends with the product **P(N)-*E*** with progress on the kinetic path of **I(N)**.

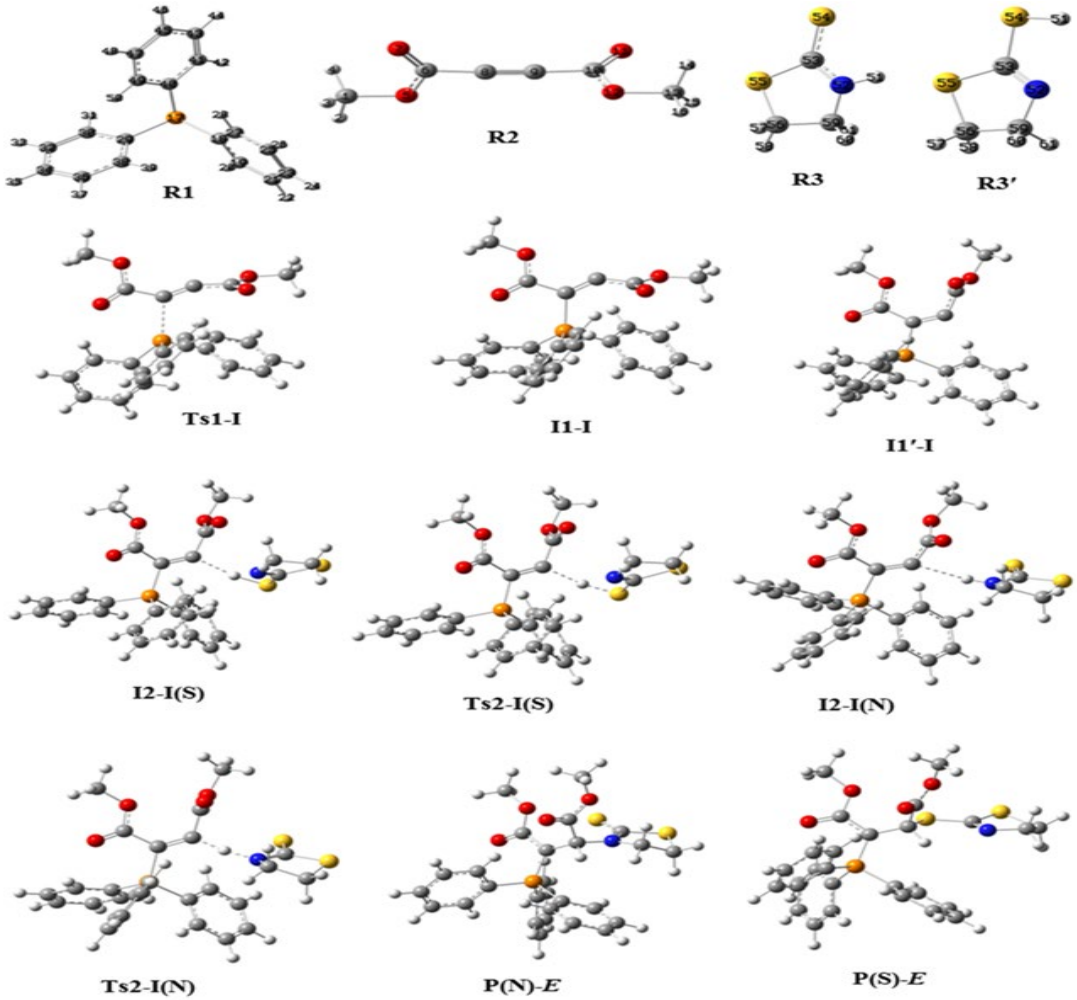

Figure 2. Optimized structures (including reactants, intermediates, transition states, and products) the reaction path **I** at B3LYP/6-311++G(d,p) level in the gas phase

The overall process in pathway **II** is similar to pathway **I**. The difference is that one of COOMe groups has a different orientation with similar structures on pathway **I**, and this path leads to a product *Z*- configuration (**P(N)-*Z*** and **P(S)-*Z***). A comparison of the energy levels in kinetic pathways **I** and **II** in Fig. **4** shows that all structures, including transition states and intermediates and products, in kinetic pathway **I** are more stable than pathway **II**. The energy barrier of the first step is equal to 122.01(113.19) kJ/mol which is higher than path **I**. Because the first step in both paths **I** and **II** with the highest energy barrier is known as the rate-determining step, so kinetic path **I** have a kinetic preference over path **II**. The second step of this kinetic path, like the path **I**, has two competitive paths **II(N)** and **II(S)**. As can be seen in Fig. **4**, competitive path **II(S)** has a much lower energy barrier (2.26 (1.32) kJ/mol) than competitive Path **II(N)** (25.81 (23.61) kJ/mol), but progress on kinetic path **II(S)** requires crossing a tautomerism energy barrier with the high value of 115.72 (115.07) kJ/mol. Like kinetic path **I**, it prefers the reaction with a lower energy barrier of 27.20 (19.59) kJ/mol in structure **Ts-II(N)** compared to a high energy barrier of the tautomeric process by the

value of 115.72 (115.07). In the last step, the reaction prefers the formation of S54-C9 bond compared to N52-C9, to achieve a more stable product **P(S)-*Z***. At this step, the reaction is completely selective in the formation of the N52-C9 bond, so that the final products of the reaction are only a mixture of **P(N)-*E*** and **P(N)-*Z*** [26]. In the synthesis of stable phosphorus ylide in the presence of 2-mercapto thiazoline, **P(N)-*E*** is known as the major isomer (94%) over **P(N)-*Z*** [26]. The result can have several reasons that can be evaluated theoretically. Therefore, we will analyze the theoretical results in detail to find out the majority of **P(N)-*E***.

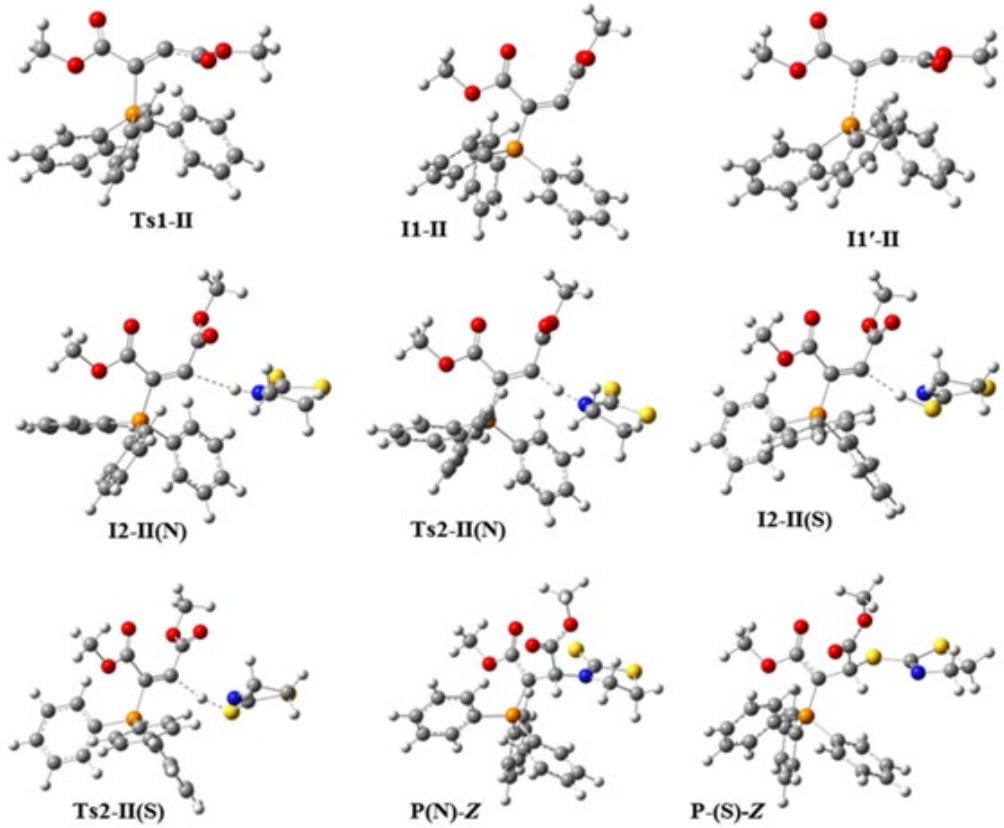

Figure 3. Optimized structures (including reactants, intermediates, transition states, and products) the reaction path **II** at B3LYP/6-311++G(d,p) level in the gas phase

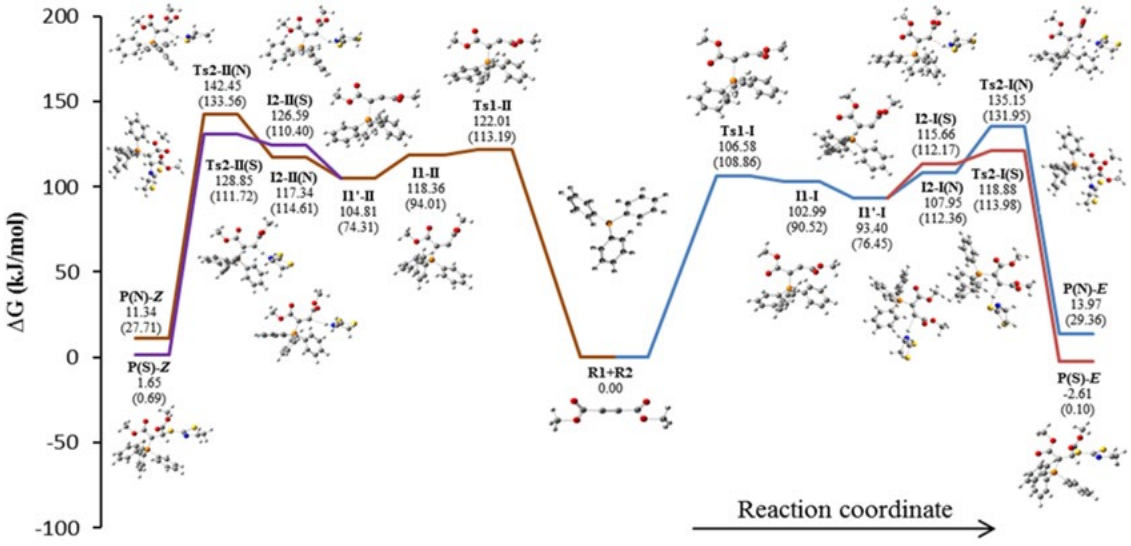

Figure 4. The energy diagram of the reaction for the two pathways **I** and **II** (data for solvent are reported in parentheses)

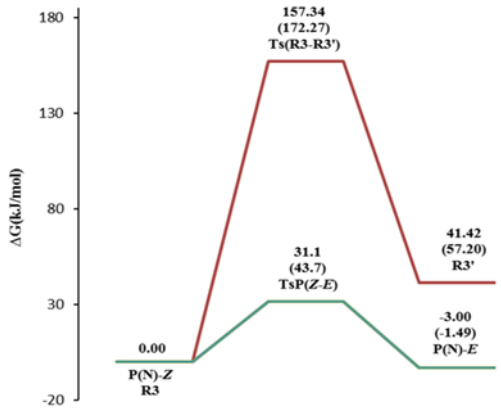

Figure 5. Potential energy diagram of transformations of **R3→R3'** and **P(N)-*Z*→P(N)-*E***

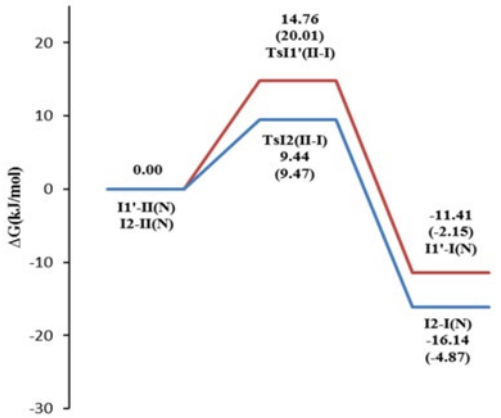

Figure 6. Potential energy diagram of transformations of **I1'-II(N)→I1'-I(N)** and **I2-II(N)→I2-I(N)**

As can be seen from Fig. **4**, the energy barrier of the first step if path **I** is lower than path **II** with an amount of 15.43 (4.33) kJ/mol. This amount of difference in the energy barrier of the first step, as the rate-determining step, can be one of the factors for further progress of the reaction in the kinetic path **I** compared to path **II**. Due to the kinetic preference of path **I**, it is obvious that the reaction prefers path **I** over path **II** to produce the product **P(N)-*E*** over **P(N)-*Z***, but this amount of difference in the energy barrier can't be the main reason for the 94% majority of **P(N)-*E*** over **P(N)-*Z***. Another factor that can lead to the preference of **P(N)-*E*** is the conversion **P(N)-*Z*** to **P(N)-*E***. The unstable product **P(N)-Z** will likely change to the stable product **P(N)-*E*** by rotating around the O-C-C-P dihedral angle. The scanning results in Fig. **5** show that process of transforming **P(N)-*Z*** to **P(N)-*E*** requires an energy barrier of 31.1(43.7) kJ/mol. Although crossing this energy barrier to achieve low stability of -3.00(-1.49) kJ/mol is not desirable in terms of kinetics and thermodynamics, but it is not impossible. Therefore, it could be one of the reasons for the preference of product **P(N)-*E*** over **P(N)-*Z***.

Along path **II**, **I1'-II(N)** may turn into **I1'-I(N)** or **I2-II(N)** turns into **I2-I(N)** as the more stable structures, and this task is accomplished by passing through potential energy barriers of 14.76(20.01) and 9.44(9.47) kJ/mol, respectively to achieve the stability of -11.41(-2.15) and -16.14(-4.87) kJ/mol (Fig. **6**). In these transformations, the reaction can continue on the path **I** and ends at **P(N)-*E*** and can be another reason for the majority of this product.

Potential energy levels in the solution phase

To examine the effect of solvent on potential energy levels, solvent phase computations were conducted for acetone with a dielectronic constant of (ε= 20.7) using the CPCM model. Potential energy levels are shown in Fig. **4** for two pathways **I** and **II** in acetone. The results show that the energy levels in the solution phase are reduced compared to the gas phase, except in four cases. The rate of decrease in energy level in path **II** is greater than in path **I**. Examination of results in the solvent phase

indicates that the energy barrier of the first step of the reaction is significantly higher than the second step in pathways **I** and **II**. Thus, similar to the gas phase, the first step of the reaction is known as the rate-determining step. Due to the less energy barrier of the first step in pathway **I**, this path is kinetically preferred to path **II**. The energy barrier of the transformation of **P-*Z*** to **P-*E*** is increased as much as 12.6 kJ/mol (Fig. **5**). The energy barrier of the transformation of **I1'-II** to **I1'-I** increased as much as 5.25 kJ/mol and the energy barrier of **I2-II** to **I2-I** transformation has remained almost unchanged compared to the gas phase (Fig. **6**). It should be noted that the difference between the energy barrier of the first step (as the rate-determining step) in the two pathways **I** and **II** phases has been significantly reduced compared to the gas. As the difference of the energy barrier in the two pathways decreases from 15.43 kJ/mol in the gas phase to 4.33 kJ/mol in the solution phase.

Natural bond orbital analysis (NBO)

Analysis of the atomic charge of atoms participating in the reaction mechanism was conducted by NBO analysis and results are given in Table **1**.

Table 1. Atomic charge of some important structures participating in both paths **I** and **II**

atom	charge	atom	charge	atom	charge	atom	charge
R1		**R2**		**R3**		**R3′**	
qP(17)	0.844	qO(7)	-0.545	qH(51)	0.406	qH(51)	0.147
qC(18)	-0.329	qC(8)	-0.008	qS(54)	-0.112	qS(54)	0.073
qC(29)	-0.329	qC(9)	-0.034	qC(53)	-0.107	qC(53)	-0.042
qC(40)	-0.329	qC(10)	0.733	qN(52)	-0.630	qN(52)	-0.518
qC(6)	0.731	qO(11)	-0.545	qS(55)	0.299	qS(55)	0.224
$R3^-$				**I1-I**			
qS(55)	0.081			qC(6)	0.795	qO(11)	-0.664
qC(53)	-0.026			qO(7)	-0.648	qP(17)	1.499
qS(54)	-0.417			qC(8)	-0.525	qC(18)	-0.376
qN(52)	-0.609			qC(9)	-0.082	qC(29)	-0.378
				qC(10)	0.662	qC(40)	-0.370
Ts1-I				**I1-II**			
qC(6)	0.742	qO(11)	-0.616	qC(6)	0.793	qO(11)	-0.667
qO(7)	-0.616	qP(17)	1.193	qO(7)	-0.572	qP(17)	1.512
qC(8)	-0.152	qC(18)	-0.370	qC(8)	-0.548	qC(18)	-0.375
qC(9)	-0.118	qC(29)	-0.362	qC(9)	-0.077	qC(29)	-0.382
qC(10)	0.695	qC(40)	-0.355	qC(10)	0.659	qC(40)	-0.370
Ts1-II				**P(N)-*E***		**P(N)-*Z***	
qC(6)	0.762	qO(11)	-0.626	qC(8)	-0.731	qC(8)	-0.746
qO(7)	-0.564	qP(17)	1.239	qC(9)	-0.096	qC(9)	-0.088
qC(8)	-0.280	qC(18)	-0.371	qP(17)	1.629	qP(17)	1.626
qC(9)	-0.076	qC(29)	-0.368	qH(51)	0.234	qH(51)	0.230
qC(10)	0.690	qC(40)	-0.358	qS(52)	-0.123	qS(52)	-0.117
				qN(61)	-0.520	qN(61)	-0.520

Evaluation of results of path **I** in Table **1** indicates that atom P17 has an atomic charge of 0.844 a.u. and atoms C18, C29 and C40 have the same atomic charges of -0.329 a.u. This result is indicative of the high polarity of C-P bonds in **R1**. In the structure **Ts1-I**, the amount of atomic charge of P17 has decreased to 1.193 a.u. Although the electronic charge of atoms C18, C29, and C40 in **Ts1-I** are increased slightly, it doesn't seem to be the reason for the reduction in the electronic charge of atom P17. By the formation of the P17-C8 bond in the structure **I1-I**, the electronic charge of atom P17 is decreased to the amount of 1.499 a.u. It is expected that with the formation of the P17-C8 bond, the electron density of bond C8≡C9 will be concentrated on atom C9. The electronic charge of atom C9 in **I1-I** shows that the charge of this atom increased slightly in comparison to **R2** from -0.034 a.u to -0.082 a.u, while, the electronic charge of atom C8 increased significantly as much as -0.517 a.u. This result shows that the P17-C8 bond in the **I1-I** structure is strongly polar.

The amount of charge transfer from **R1** to **R2** in **Ts1-I** is equal to -0.452 a.u, which is increased to -0.879 a.u by the formation of the P17-C8 bond in **I1-I**. By rotating the dihedral angle in **I1'-I**, the charge transfer increases to -0.965 a.u, thus increasing the charge concentration on atoms C8 and C9. Values of charge transfer in **Ts1-I** and **Ts1-II** structures are equal to -0.452 a.u and -0.514 a.u, respectively, and are indicative of an increase in charge transfer in **Ts1-II** compared to the **Ts1-I** structure. This amount of increase in charge transfer is directly related to the charge reduction of atom P17 in **Ts1-II** compared to **Ts1-I** structure, and this could be due to the decrease in the steric factor of the **Ts1-II** structure and establishment of a stronger interaction of P17…C8. The reduction of P17…C8 bond length in **Ts1-II** (2.240 Å) compared to **Ts1-I** (2.299 Å) attests to this truth. The more polarity of the C-P bond can be an important reason for the instability of structures **Ts1-II** and **I1-II** compared to similar structures in the kinetic path **I**. Evaluations of the electronic charge of atoms in **P(N)-*E*** and **P(N)-*Z*** structures show the high polarity of the P17-C8 bond. The polarity of this bond in **P(N)-*Z*** is slightly more than **P(N)-*E***.

The bond length of P17-C8 in the **P(N)-*E*** structure is equal to 1.739 Å, which is slightly decreased to 1.734 Å in **P(N)-*Z***. The polarity of bond C-P is almost identical in both structures **P(N)-*E*** and **P(N)-*Z***. Evaluations of the electronic charges of other atoms in structures **P(N)-E** and **P(N)-Z** are not indicative of significant changes in the electronic charges of these atoms. These pieces of evidence results indicate that the rotation of the COOMe functional group has no effect on the electronic charge and as a result, there is no significant change in the potential energy. Electrostatic potential (ESP) provides a visual representation of the electron density regions of the title molecule [48, 49]. ESP map gives a surface analysis on the maximum and minimum charged regions throughout the surface of the molecule. It is a very useful descriptor for predicting favorable sites of electrophilic and nucleophilic reactions or revealing preferential sites of electrostatically dominated non-covalent interactions [50,51]. It is very intuitive from this figure to examine potential reactive sites, the blue region implies a possible site for an electrophilic attack, while the red region is expected to be a vulnerable site for nucleophilic attack. The average value of local maxima and minima of ESP for some important atoms is represented in Table **2**. The ESP-mapped van der Waals (vdW) surfaces are shown in Fig. **7**. Moreover, the changes in the average value of MEP of different atoms in **R3**, **R3',** and **R3**$^-$ are presented in Fig **8**. Atom N52 with an atomic charge of -0.630 a.u and atom H51 with an atomic charge of 0.406 a.u in structure **R3** (Table **1**) indicate a completely polar N-H bond. Conversely in structure **R3'**, atom S54 with an atomic charge of 0.224 a.u and atom H51 with an atomic charge of 0.147 a.u indicate a completely non-polar S-H bond. This result is due to the smaller radius, more hardness, and more electronegativity of atom N52 than S54, which causes more acidity of atom H51 in structure **R3** than **R3'**. The electrostatic potential values in Table **2** show the electrostatic potential of H51 in two structures **R3** than **R3′** equal to 16.34 and 6.950 kJ/mol, respectively. It is expected that H51 in **R3** with more electrostatic potential than that of **R3′** and to be a better site for nucleophilic attack. The electrostatic potential value of C9 is -38 kJ/mol and implies a possible site for an electrophilic attack of H54. The amount of electrostatic potential of atoms S54 and N52 in structure **R3**$^-$ has increased significantly compared to structures **R3** and **R3'** and has reached -115.99 and -118.31 kJ/mol, respectively.

Table 2. The average value of local maxima and minima of ESP for **R3**, **R3'** and **R3**$^-$

atom	R3	R3′	R3$^-$
S54	-22.54	-6.130	-115.99
C53	-8.30	-4.820	-112.44
N52	-0.88	-17.890	-118.31
H51	16.34	6.950	---
C61	19.76	9.620	-75.38
C60	25.62	9.660	-69.62
C57	16.72	13.5	-70.6
C58	21.70	13.51	-63.31
S55	-7.20	-6.31	-98.2

Although this difference is not significant, the higher nucleophilicity of atom N52 could be another factor, in addition to the kinetic preference of pathways **I(N)** or **II(N)**, in the preference of product **P(N)-*E*** or **P(N)-*Z*** over **P(S)-*E*** or **P(S)-*Z***. Given that products **P(N)** and **P(S)** are not convertible to each other, so the results show well

that the production of products **P(N)-*E*** and **P(N)-*Z*** are kinetically controlled.

Reaction rate

According to the results, the first step of the reaction was recognized as the rate-determining step. According to this, the mechanism of the reaction could be suggested in Fig. 9 according to kinetic evidence.

Using the approximation of the rate-determining step we will have:

$$rate = \frac{d[P]}{dt} = k_3[N^-][I2] \quad (1)$$

$$\frac{d[I1]}{dt} = k_1[R1][R2] = -k_2[I1][R3] \quad (2)$$

$$\frac{d[N^-]}{dt} = k_2[R3][I1] = -k_3[N^-][I2] \quad (3)$$

$$[N^-][I2] = \frac{k_2[R3][I1]}{-k_3} \quad (4)$$

$$rate = k_1[R1][R2] \quad (5)$$

This rate equation well displays that the overall reaction rate constant is independent of the concentration of reactant **R3** and depends only on the concentration of reactants **R1** and **R2**, which is consistent with the results of kinetic studies [52-56]. According to the conventional transition state theory (CTST), the values of the rate constant *k*(T) for elementary bimolecular reactions in the gas phase are expressed by;

$$k = \kappa\sigma \frac{k_B T}{h} \frac{Q_{TS}}{Q_R} exp\left[-(E_{TS} - E_R)/_{RT}\right] \quad (6)$$

Where the QTS and QR are the partition functions of the transition states and the reactants, kB is the Boltzmann constant, κ is the transmission coefficient. The ETS and ER are energies of the transition state and the reactants with zero-point energy correction involved. The tunneling corrections were expressed as the ratio of the quantum–mechanical to classical barrier crossing rate, assuming an unsymmetrical, one-dimensional Eckart function barrier [58]. The overall reaction rate constant was calculated using equation (5). The rate constant of the first step of the reaction as the overall reaction rate constant at 298.15 K for the pathways I and II are equal to 5.36×10-26 and 1.06×10-28 $cm^3.molecule^{-1}.s^{-1}$, respectively.

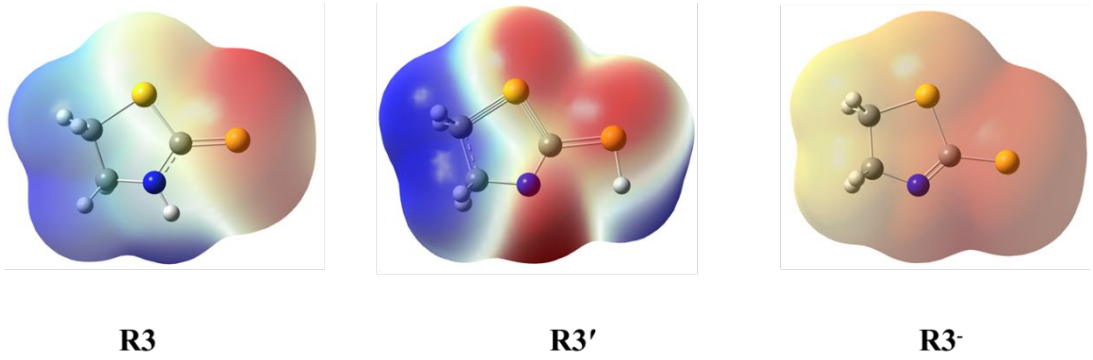

R3 **R3′** **R3⁻**

Figure 7. ESP-mapped molecular vdW surface of **R3**, **R3'** and **R3⁻**

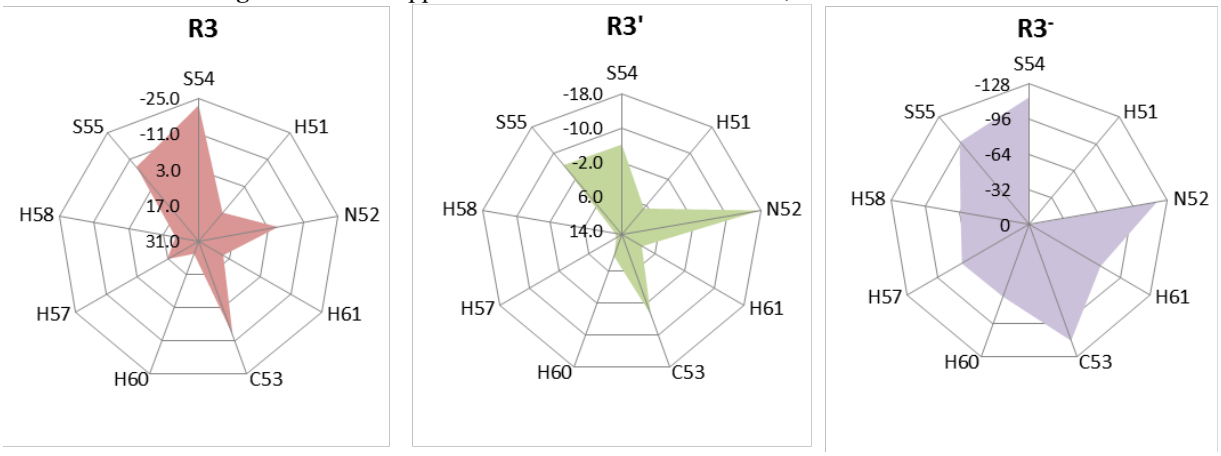

Figure 8. The changes in the average value of ESP in **R3**, **R3'** and **R3⁻**

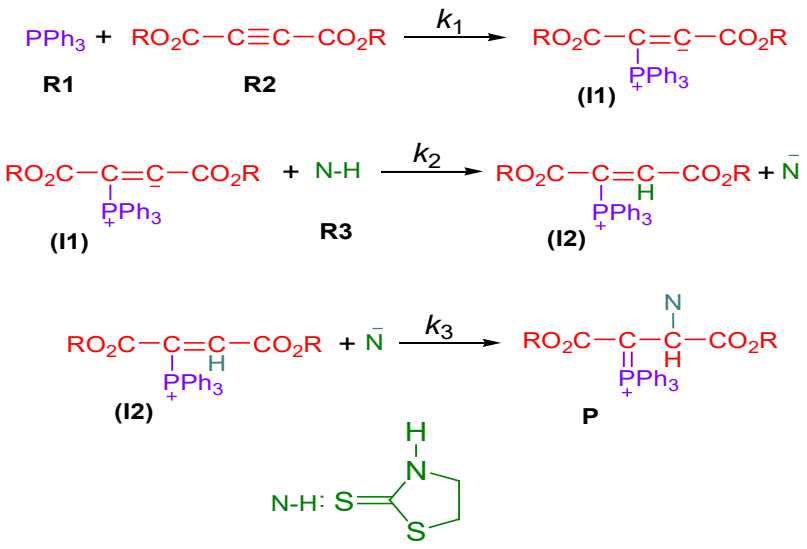

Figure 9. The reaction mechanism between triphenylphosphine and dimethyl acetylenedicarboxylate in the presence of 2-mercapto thiazoline

4. Conclusions

The mechanism of the reaction between triphenylphosphine R1, dimethyl acetylenedicarboxylate R2, and 2-mercapto thiazoline R3 as NH-acid for the production of phosphorus ylide with two different E- and Z-rotamers was examined theoretically and the results were obtained as follow:

1- Two different pathways I and II were established in the reaction mechanism by the nucleophilic proximity of P17 in triphenylphosphine R1 to the C8 in dimethyl acetylenedicarboxylate R2 in different directions.

2- According to the potential energy diagrams, the overall reaction in each pathway consists of two steps that pass through two energy barriers with transition states of Ts1 and Ts2.

3- The first step of the reaction has been known as the rate-determining step. Based on this result, the reaction rate equation was obtained and the overall rate constant was calculated.

4- Pathway I by possessing a lower energy barrier is more kinetically desirable than pathway II, and so the reaction proceeds through this pathway.

5- Despite the same thermodynamic stability, theoretical calculations were well able to explain the reason for the dominant of product P(N)-E over P(N)-Z, and kinetic preference is the preference factor of P(N)-E.

6- Although in solution, the potential energy levels in some cases were accompanied by significant changes, the overall results such as rate-determining step, the stability of a specific isomer of the product, preference of a kinetic path, and other results obtained are the same as the results obtained in the gas phase.

7- The overall rate equation obtained shows the overall reaction rate constant depends on the concentration of R1 and R2 without dependence on the concentration of R3.

8- The kinetic preference of path I over path II, the conversion of intermediates with a Z- to E-configuration along the kinetic path, and the high energy barrier of the P(N)-E to P(N)-Z conversion are the three main reasons for the preference of P(N)-E over P(N)-Z, which is obtained using quantum computing.

References

[1] B. Balali-Mood, Chemistry and classification of OP compounds, in Basic and Clinical Toxicology of Organophosphorus Compounds, " Springer, London, UK, 2014.

[2] S. Kumar, G. Kaushik, J.F Villarreal-Chiu, Environmental Science and Pollution Research, 2016, 23, 9480.

[3] A.W Johnson, Ylide Chemistry, Academic Press: London, 1966.

[4] J.I.G. Cadogan, Organophosphorus Reagents in Organic Synthesis, Academic Press: New York, 1979.

[5] R. Engel, Synthesis of Carbon-Phosphors Bonds; CRC Press: Boca Raton, FL, 1988.

[6] H.R. Hudson, In The Chemistry of Organophosphorus Compounds; Primary, Secondary, and Tertiary Phosphates and Heterocyclic Organophosphorus(III) Compounds, Wiley, New York, 1990.

[7] V. Iaroshenko, Organophosphorus Chemistry: From Molecules to Applications, Wiley-VCH Verlag GmbH & Co. KGaA, 2019.

[8] L. Fitjer, U. Quabeck, The Wittig Reaction Using Potassium-tert-butoxide High Yield Methylenations of Sterically Hindered Ketones, Synth Commun 15 (1985) 855-864.

[9] I. Yavari, S. Ali-Asgari, K. Porshamsian, M. Bagheri, Efficient synthesis of functionalized bis-(4-oxo-1,3-thiazole-5-ylidene)acetates, Sulfur Chem 28 (2007) 477-482.

[10] A. Ramazan, A. Souldozi, Dipotassium-Hydrogen-Phosphate-Powder-Catalyzed Stereoselective C-Vinylation of Diphenylacetonitril, Phosphorus Sulfur Silicon Relat Elem 180 (2005) 2801-2804.

[11] I. Yavari, A.A. Alizadeh, A Simple Approach to the Synthesis of 1,4-Bis(arylsulfonyl)tetrahydropyrazine-2,5-diones, Monatsh Chem 134 (2003) 435-438.

[12] A. Ramazani, A. Bodaghi, One-pot, four-component synthesis of dialkyl [indane-1,3-dione-2-ylidene]alkoxysuccinates, Tetrahedron Lett 41 (2000) 567-568.

[13] A. Hassanabadi, M. Anary-Abbasinejad, A. Dehghan, Three-Component Reaction of Triphenylphosphine, Dimethyl Acetylenedicarboxylate, and Aldehyde Benzoylhydrazones: An Efficient One-Pot Synthesis of Stable Phosphorus Ylides, Synth Commun 39 (2009) 132-138.

[14] S.M. Habibi-Khorassani, M.T. Maghsoodlou, A. Ebrahimi, M. Kazemian, S. Salari, S. Nasiri, 1H NMR Kinetic Investigation of the Equilibrium between the Z- and E-Isomers in a Stable Phosphorus Ylide Involving 2-Mercaptobenzimidazole, Prog React Kinet Mech 38 (2013) 295-304.

[15] I. Yavari, M. Adib, F. Jahani-Mogaddam, M.H. Sayahi, A Simple Synthesis of Stable Heterocyclic Phosphorus Ylides Derived from NH-Acids, Phosphor Sulfur Silicon Relat Elem 177 (2002) 545-553.

[16] M.R. Islami, I. Yavari, A.M. Tikdari, L. Ebrahimi, S. Razee, H.R. Bijanzadeh, A Practical Method for Synthesis of Stable Phosphorus Ylides in Aqueous, Media ChemInform 34 (2003) 124-147.

[17] M. Ziyaadini, M.T. Maghsoodlou, N. Hazeri, S.M. Habibi-Khorassani, Synthesis of New Stable Phosphorus Ylidesand 1,4-Diionic Organophosphorus Compoundfrom a Reaction between HexamethylPhosphorous Triamide and DimethylAcetylenedicarboxylate in the Presence of CH-Acids, Heteroat Chem 24 (2013) 84-89.

[18] I. Yavari, Z. Hossain, A. Alizadeh, Diastereoselective Synthesis of meso-Bisphosphonates from Trialkyl(aryl) Phosphites and Activated Acetylenes in the Presence of 4-Nitrophenol, Monatsh Chem 137 (2006) 1083-1088.

[19] M.T. Maghsoodlou, N. Hazeri, S.M. Habibi-Khorassani, A. Ghulame-Shahzadeh, M. Nassiri, Simple Synthesis of Stable Phosphorus Ylides from Indole and Some of Its Derivatives, Phosphor Sulfur Silicon Relat Elem 18 (2006) 913-919.

[20] M.T. Maghsoodlou, R. Heydari, S.M. Habibi-Khorassani, M.K. Rofouei, M. Nassiri, E. Mosaddegh, A. Hassankhani, Chemoselective synthesis of phosphorus ylides through the reaction of 2-mercaptobenzimidazole and 2-hydroxybenzimidazole with triphenylphosphine and acetylenic esters, Sulfur Chem 27 (2006) 341-346.

[21] S.M. Habibi-Khorassani, T. Maghsoodlou, A. Ebrahimi, M. Zakarianejad, M. Fattahi, Kinetics and Mechanism of the Reactions Between Triphenylphosphine, Dialkyl Acetylenedicarboxilates and an NH-Acid, Pyrazole, by UV, Spectrophotometry Solution Chem 36 (2007) 1117-1127.

[22] M. Zakarianezhad, B. Makiabadi, S.S. Hosseini, Theoretical study of the reaction mechanism between triphenylphosphine with dialkyl acetylenedicarboxylates in the presence of benzotriazole, Theor Chem Acc 140 (2021) 13-25.

[23] M. Moradian, S.M.H. Khorassani, M.T. Maghsoodlou, A. Ebrahimi, M. Zakarianezhad, P. Karimi, Kinetic and Mechanism Investigation of the Reactions of Triphenylphosphine, Dialkyl Acetylenedicarboxylates and NH-Acids by Ultra Violet, Asian J Chem 21 (2009) 1069-1080.

[24] S.M. Habibi-Khorasani, A. Ebrahimi, M.T. Maghsoodlou, S. Same-Salari, S. Nasiri, H. Ghasempour, Dynamic 1H NMR study around the carbon–carbon single bond and partial carbon–carbon double bond in the two particular phosphorus ylides and in an enaminoester, Magn Reson Chem 49 (2011) 213–220.

[25] R. Kabiri, N. Hazeri, S.M. Habibi-Khorasani, M.T. Maghsoodlou, A. Ebrahimi, L.

Saghatforoush, G. Marandi, Z. Razmjoo, Synthesis, dynamic 1H NMR and theoretical study of aryl-nitrogen single bond rotational energy barriers in highly functionalized 4H-chromenes, Arkivoc xvii (2008) 12-19.

[26] M.T. Maghsoodlou, N. Hazeri, S.M. Khorassani, M. Nassiri, G. Marandi, G. Afshari, U. Niroumand, An efficient synthesis of stable sulfurcontaining phosphoranes derived from 2-mercapto-1-methylimidazole and 2-thiazoline-2-thiol, J Sulfur Chem 26 (2005) 261-266.

[27] S.M. Habibi-Khorassani, A. Ebrahimi, M.T. Maghsoodlou, H. Saravani, M. Zakarianezhad, M. Ghahramaninezhat, M.A. Kazemian, M. Nassiri, Z. Khajehali, Theoretical study, an efficient synthesis route to, and kinetic investigation of, stable phosphorus ylides derived from benzamide, Prog React Kinet Mech 34 (2009) 261-288.

[28] M. Zakarianezhad, P. Mohammad Dadi, Mechanistic investigation of the reaction of thiourea with dialkyl acetylenedicarboxylates: A theoretical study Sulfur Chem., 2015, 36, 422-433.

[29] M. Zakarianezhad, S.M. Habibi-Khorassani, A. Ebrahimi, M.T. Maghsoodlou, H. Ghasempour, NMR study, theoretical calculations for assignment of the Z- and E-isomers, and kinetics investigation of stable phosphorus ylides involving a 2-mercapto-4,6-dimethyl pyrimidine, Heteroat Chem 21 (2010) 462-474.

[30] S.M Habibi-Khorassani, M.T. Maghsoodlou, H. Ghasempour, M. Zakarianezhad, M. Nassiri, Z. Ghahghaie, AIM analysis, synthetic, kinetic and mechanistic investigations of the reaction between triphenylphosphine and dialkyl acetylenedicarboxylate in the presence of 3-methoxythiophenol, J Chem Sci 125 (2013) 387-399.

[31] H.R. Masoodi, M. Zakarianezhad, S. Bagheri, B. Makiabadi, M. Shool, Substituent effects on some calculated NMR data in T-shapedconfiguration of benzene dimer, Chem Phys Lett 61 (2014) 143-147.

[32] M. Zakarianejad, H. Ghasempour, S.M. Habibi-Khorassani, M.T. Maghsoodlou, B. Makiabadi, M. Nassiri, Z. Ghahghayi, A. Abedi, Theoretical study, synthesis, kinetics and mechanistic investigation of a stable phosphorus ylide in the presence of methyl carbamate as a NH-acid, Arkivoc 2013 (2013) 171-190.

[33] M. Zakarianezhad, S.M. Habibi-Khorassani, M.T. Maghsoodlou, B. Makiabadi, Understanding the mechanism of stable phosphorus ylides derived from imidazole, 2-Methylimidazole or 4-Methylimidazole: A kinetic study, Orien J Chem 28 (2012) 1259-1269.

[34] D. Suárez, M. Zakarianezhad, R. López, Insights into the hydrolytic chemistry of molybdocene dichloride based on a theoretical mechanistic study, Theor Chem Acc 132 (2013) 1-11.

[35] [35] M. Zakarianezhad, S.M. Habibi-Khorassani, Z. Khajehali, B. Makiabadi, M. Feyzi, A. Taheri, Mechanistic investigation of the reaction between triphenylphosphine, dialkyl acetylenedicarboxylates and pyridazinone: A theoretical, NMR and kinetic study, Reac Kinet Mech Catal 111 (2014) 461-474.

[36] H.R. Masoodi, S. Bagheri, M. Mohammadi, M. Zakarianezhad, B. Makiabadi, The influence of cation-Π and anion-Π interactions on some NMR data of s-triazine. HF hydrogen bonding: A theoretical study, Chem Phys Lett 588 (2013) 31-36.

[37] H. Roohi, A.R. Nowroozi, A. Ebrahimi, B. Makiabadi, Effect of CH3CO functional group on the molecular and electronic properties of BN43zz nanotube: A computational chemistry study, J Mol Struct 952 (2010) 36-45.

[38] H. Roohi, B. Mackiabadi, Conformations of O3-F 1:1 complexes. an Ab initio study, Bull Chem Soc Jpn 80 (2007) 1914-1919.

[39] B. Makiabadi, H. Kian, The hydrogen bond interactions in glycine-nitrosamine complexes: A DFT study, Monatsh Chem 146 (2015) 69-78.

[40] B, Makiabadi, Z.A. Tajaddini, Theoretical Investigation of Proton Transfer in Thiazolidine-2-thione and Oxazolidine-2-thione via Direct Transition and Self-Assisted and Water-Assisted Tautomerization, Chem Heterocycl Compd 51 (2015) 361-369.

[41] M. Frisch, G. Trucks, H.B. Schlegel, G. Scuseria, M. Robb, J. Cheeseman, G. Scalmani, V. Barone, B. Mennucci, G, Petersson, Gaussian 09, Revision A. 02, Gaussian. Inc, Wallingford, CT, 2009.

[42] C. Gonzalez, H.B. Schlegel, Reaction path following in mass-weighted internal

coordinates, J Phys Chem 94 (1990) 5523-5527.

[43] C. Gonzalez, H.B. Schlegel, An improved algorithm for reaction path following, J Chem Phys 90 (1989) 2154.

[44] J. Tomasi, M. Persico, Molecular Interactions in Solution: An Overview of Methods Based on Continuous Distributions of the Solvent, Chem Rev 94 (1994) 2027-2094.

[45] E. Cances, B. Mennucci, A new integral equation formalism for the polarizable continuum model: Theoretical background and applications to isotropic and anisotropic dielectrics, J Tomasi J Chem Phys 107 (1997) 3032-3041.

[46] M. Cossi, V. Barone, R. Cammi, J, Tomasi, Ab initio study of solvated molecules: a new implementation of the polarizable continuum model, Chem Phys Lett 255 (1996) 327-355.

[47] D.E. Glendening, A.E. Reed, J.E. Carpenter, F. Weinhold, NBO, Version 3.1.

[48] J.S. Murray, P. Politzer, Electrostatic potentials: chemical applications,in: Schleyer PvR (Ed.),Encyclopedia of Computational Chemistry, Wiley, West Sussex, 1998, 912-920.

[49] J.S. Murray, K. Sen, Molecular Electrostatic Potentials: Concepts and Applications, Elsevier, Amsterdam, 1996.

[50] T. Lu, S. Manzetti, Wavefunction and reactivity study of benzo [a] pyrene diol epoxide and its enantiomeric forms, J Struct Chem 25 (2014) 1521-1533.

[51] B.P.S. Gautam, M. Srivastava, R.L. Prasad, R.A. Yadav, Synthesis, characterization and quantum chemical investigation of molecular structure and vibrational spectra of 2, 5-dichloro-3,6-bis-(methylamino)1,4-benzoquinone, Spectrochim Act A Mol Biomol Spectrosc 129 (2014) 241-254.

[52] M. Zakarianezhad, B. Makiabadi, M. Shool, Experimental and theoretical study of stable phosphorus ylides derived from indazole in the presence of different dialkyl acetyelenedicarboxylates: Further insights into the reaction mechanism, J Chil Chem Soc 61 (2016) 2929-2934.

[53] S.M. Habibi-Khorassani, M.T. Maghsoodlou, A. Ebrahimi, H. Roohi, M. Zakarianezhad, M. Moradian, Kinetic investigation of the reactions between triphenylphosphine, dialkyl acetylenedicarboxylates and SH-acid such AS 2-thiazoline-2-thiol or 2-mercaptobenzoxazole by UV spectrophotometry, Prog React Kinet 30 (2005) 127-144.

[54] S.M. Habibi Khorassani, M.T. Maghsoodlou, A. Ebrahimi, H. Roohi, M. Zakarianezhad, H.R. Dasmeh, P Kinetic investigation of the reaction between triphenylphosphine, dialkyl acetylenedicarboxylate, and carbazole by the UV spectrophotometry technique, Phosphorus Sulfur Silicon Relat Elem 181 (2006)1103-1115.

[55] H. Ghasempour, M. Zakarianezhad, B. Makiabadi, S.M. Habibi-Khorassani, Mechanism investigation of stable phosphorus ylides derived from saccharine in the presence of different dialkyl acetylenedicarboxylates: Experimental and theoretical study, Iran J Sci Technol Trans A Sci 40 (2016) 255-265.

[56] M. Zakarianezhad, B. Makiabadi, P. Sotoodeh, E. Zeydabadi, Investigation of the reaction mechanism between cyclohexyl isocyanide and dimethyl acetylenedicarboxylate in the presence of 2-mercaptobenzoxazole: a theoretical study, Phosphorus Sulfur Silicon Relat Elem 196 (2021) 656-663.

[57] M. Zakarianezhad, S.M. Habibi-Khorassani, M.T. Maghsoodlou, B. Makiabadi, H. Ghasempour, Understanding the mechanism of stable phosphorus ylides derived from maleimide: A kinetic study, Iran J Sci Technol Trans A Sci 36 (2012) 251-258.

[58] C, Eckart, The Penetration of a Potential Barrier by Electrons, Phys Rev 35 (1930) 1303-1309.